THE JOURNAL OF BIOLOGICAL CHEMISTRY
Vol. 280, No. 11, Issue of March 18, pp. 10395–10402, 2005
Printed in U.S.A.

Cytochrome b_6 Arginine 214 of *Synechococcus* sp. PCC 7002, a Key Residue for Quinone-reductase Site Function and Turnover of the Cytochrome *bf* Complex*

Received for publication, September 23, 2004, and in revised form, December 9, 2004
Published, JBC Papers in Press, January 4, 2005, DOI 10.1074/jbc.M410948200

Matthew E. Nelson‡, Giovanni Finazzi§, Qing Jun Wang¶‖, Kelly A. Middleton-Zarka‡, John Whitmarsh¶‡‡, and Toivo Kallas‡§§**

From the ‡Department of Biology and Microbiology, University of Wisconsin-Oshkosh, Oshkosh, Wisconsin 54901, §Physiologie Membranaire et Moléculaire du Chloroplaste, CNRS UPR 1261, Institut de Biologie Physico-Chimique, 13 Rue Pierre et Marie Curie, 75005 Paris, France, and the ¶Center of Biophysics and Computational Biology, University of Illinois, Urbana, Illinois 61801

Quinone-reductase (Q_i) domains of cyanobacterial/chloroplast cytochrome *bf* and bacterial/mitochondrial *bc* complexes differ markedly, and the cytochrome *bf* Q_i site mechanism remains largely enigmatic. To investigate the *bf* Q_i domain, we constructed the mutation R214H, which substitutes histidine for a conserved arginine in the cytochrome b_6 polypeptide of the cyanobacterium *Synechococcus* sp. SPCC 7002. At high light intensity, the R214H mutant grew ~2.5-fold more slowly than the wild type. Slower growth arose from correspondingly slower overall turnover of the *bf* complex. Specifically, as shown in single flash turnover experiments of cytochrome b_6 reduction and oxidation, the R214H mutation partially blocked electron transfer to the Q_i site, mimicking the effect of the Q_i site inhibitor 2-*N*-4-hydroxyquinoline-*N*-oxide. The kinetics of cytochrome b_6 oxidation were largely unaffected by hydrogen-deuterium exchange in the mutant but were slowed considerably in the wild type. This suggests that although protonation events influenced the kinetics of cytochrome b_6 oxidation at the Q_i site in the wild type, electron flow limited this reaction in the R214H mutant. Redox titration of membranes revealed midpoint potentials ($E_{m,7}$) of the two *b* hemes similar to those in the wild type. Our data define cytochrome b_6 Arg^{214} as a key residue for Q_i site catalysis and turnover of the cytochrome *bf* complex. In the recent cytochrome *bf* structures, Arg^{214} lies near the Q_i pocket and the newly discovered c_i or *x* heme. We propose a model for Q_i site function and a role for Arg^{214} in plastoquinone binding.

The cytochrome *bf* complex of oxygenic photosynthesis transfers electrons between the photosystem II and I reaction centers. The functional complex is a dimer comprising four major subunits (1, 2): the Rieske iron-sulfur protein (ISP)[1] with a 2Fe-2S cluster; cytochrome *f*, which binds a *c*-type heme; and cytochrome b_6, which binds high and low potential *b* hemes, b_H and b_L, and a "subunit IV" (3–6). Four or five additional small subunits, PetG, PetL, PetM, PetN, and PetO (in chloroplasts) have also been evidenced (reviewed in Refs. 7 and 8). In addition, the recent x-ray crystal structures of cytochrome *bf* complexes have revealed a previously undetected and unique heme designated heme *x* in the cyanobacterium *Mastigocladus laminonsus* (9) or heme c_i in the alga *Chlamydomonas reinhardtii* (10). This extra heme, a chlorophyll, and a carotenoid molecule/monomer of the complex are features that distinguish cytochrome *bf* complexes from the related, bacterial/mitochondrial cytochrome *bc* complexes (Refs. 9 and 10; see also Refs. 11 and 12 for reviews).

Cytochrome *bf* complexes couple proton translocation across the membrane to electron transfer from a lipophilic, two-electron donor (plastoquinol) to a hydrophilic, one-electron acceptor protein (plastocyanin or a *c*-type cytochrome). The most widely accepted model to explain the mechanism of *bc*-*bf* complexes is the "Q cycle" hypothesis of Mitchell (13). This scheme, as modified by Crofts *et al.* (14) and others (for example see Ref. 15), postulates both an oxidation of plastoquinol and a reduction of plastoquinone at two distinct sites within the protein, the Q_o and Q_i sites, located on opposite, positive and negative sides of the membrane. Plastoquinol oxidation at the Q_o site involves transfer of electrons to both a high potential chain (the Rieske ISP, cytochrome *f*, and plastocyanin or cytochrome c_6) and a low potential chain (hemes b_L and b_H and plastoquinone at the Q_i site) as illustrated in Fig. 1. Plastoquinol oxidation releases two protons into the lumen, and plastoquinone reduction at the Q_i site picks up two protons from the stromal space (reviewed in Refs. 5, 11, 12, and 16).

Structural elucidation of mitochondrial cytochrome *bc* complexes by x-ray crystallography has suggested a mechanism for plastoquinol oxidation at the Q_o site (Refs. 17–20; see also Ref. 21). The extramembrane, cluster-binding domain of the Rieske protein assumes different conformations with respect to its transmembrane helix (18–20, 22, 23). A movement of the qui-

* This work was supported by National Science Foundation Grant MCB-0091415 and University of Wisconsin-Oshkosh Faculty Development Board Grant R788 (to T. K.) and by funds from the Centre National de la Recherche Scientifique (France). The costs of publication of this article were defrayed in part by the payment of page charges. This article must therefore be hereby marked "*advertisement*" in accordance with 18 U.S.C. Section 1734 solely to indicate this fact.

‖ Present address: Mass Spectrometry Lab, Rockefeller University, 1230 York Ave., New York, NY 10021.

** Present address: Potato Breeding and Genetics, Michigan State University, Crop and Soil Science Dept., East Lansing, MI 48824.

‡‡ Present address: NIGMS, National Institutes of Health, Center for Bioinformatics and Computational Biology, 45 Center Drive, Bethesda, MD 20892-6200.

§§ To whom correspondence should be addressed. Tel.: 920-424-7084; E-mail: kallas@uwosh.edu.

[1] The abbreviations used are: ISP, Rieske iron-sulfur protein; b_L, low potential cytochrome b_6 heme; b_H, high potential cytochrome b_6 heme; c_i (*x*), heme c_i (or *x*); *f*, cytochrome *f* heme; Q_o, plastoquinol oxidation site; Q_i, plastoquinone reduction site; FCCP, cabonylcyanide-*p*-(trifluoro-methoxy)phenyl-hydrazone; NQNO, 2-*N*-4-hydroxyquinoline-*N*-oxide; MOPS, 3-[*N*-morpholino]propanesulfonic acid; Sm, streptomycin; Sp, spectinomycin.

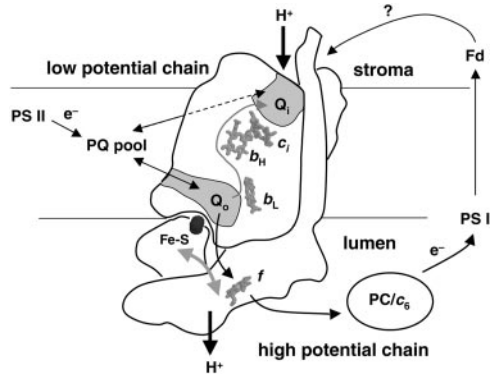

FIG. 1. **Redox centers and high and low potential electron transfer chains of the cytochrome *bf* complex.** Abbreviations: *PS II* and *PS I*, photosystems II and I; *PQ pool*, plastoquinone pool; *Fe-S*, Rieske 2Fe-2S cluster; *PC*/c_6, plastocyanin or cytochrome c_6; *Fd*, ferredoxin. The *two-headed arrow* represents the movement of the Rieske ISP cluster. In plastoquinol oxidation at the Q_o site, electrons follow high potential (Q_o > Fe-S > *f* > plastocyanin or cytochrome c_6 > PS I) and low potential (Q_o > b_L > b_H > (c_i?) > Q_i > PQ pool) pathways. The locations of the redox centers are taken from the cytochrome *bf* structures (9, 10).

nol molecule has also been predicted, based on the location within the Q_o site of residues responsible for inhibitor resistance (reviewed in Ref. 12). An interpretative model has been proposed (12), according to which the quinol and the oxidized Rieske ISP remain within hydrogen bonding distance at the Q_o site until an electron is transferred from the quinol to the Rieske ISP cluster. These partners then move apart to reduce hemes b_L and c_1 (equivalent to heme *f* in the *bf* complex), respectively. The recent three-dimensional structures of cytochrome *bf* complexes (9, 10) are compatible with this model for Q_o site function.

Less information is available on the oxidation mechanism of the b_6 hemes and reduction of plastoquinone at the Q_i site (for examples see Refs. 16 and 24–26). According to the Q cycle model, this occurs via a two-step reduction of a quinone molecule at the Q_i site. Thus, under oxidizing conditions, plastoquinol at the Q_o site reduces cytochrome b_L, which in turn reduces cytochrome b_H. A second turnover places both b_L and b_H in a reduced state causing the reduction of a plastoquinone to plastoquinol at the Q_i site and proton uptake from the stromal space. This model has been confirmed experimentally for cytochrome *bc* complexes, mainly from results obtained with the inhibitor antimycin (26–28), which binds selectively to the Q_i site (18–20). However, these results cannot be transposed directly to cytochrome *bf* complexes. Inhibitors of the cytochrome *bf* Q_i site have been identified, but none are completely effective. The inhibitor NQNO (29), which seems to operate by a mechanism similar to that of antimycin, only partially blocks electron flow (29, 30). Moreover, the redox midpoint potentials of the *b* hemes differ in *bc* and *bf* complexes (reviewed in Ref. 6). Thus, the equilibrium between heme b_H and the Q_i site quinone lies in favor of the latter in *bc* complexes and the former in cytochrome *bf* complexes (16, 25). This suggests that although two electrons can be injected consecutively onto the quinone molecule in *bc* complexes, the transfer must occur essentially in a concerted manner in cytochrome *bf* complexes (16, 25). Finally, the additional heme near the Q_i domain of *bf* complexes suggests that the mechanism of quinone reduction may be very different from that in cytochrome *bc* complexes. Based on its ligation properties, Stroebel *et al.* (10) have suggested that the new heme belongs to the family of the penta-coordinate high spin *c* hemes. Both the algal (10) and cyanobacterial (9) structures suggest that the c_i (or *x*) heme may be involved in electron flow from heme b_H to the Q_i plastoquinone and cyclic flow from photosystem I.

No functional evaluation of the cytochrome *bf* Q_i site mechanism has yet been obtained because mutations of this site have not been available from oxygenic, photosynthetic organisms. Prior to elucidation of the cytochrome *bf* crystal structures, we have initiated a molecular genetic study to probe the mechanism of quinone reduction in the cytochrome *bf* complex. Although loss-of-function mutations are not allowed in cyanobacterial *bf* complexes (reviewed in Ref. 5), the feasibility of generating stable mutations within this complex in cyanobacteria is now well established (31, 32). To dissect the catalytic mechanism of the Q_i site, we generated mutation R214H in the PetB, cytochrome b_6, polypeptide of *Synechococcus* sp. PCC 7002. This changes a conserved arginine in the cytochrome *bf* complex to a histidine that is the conserved, corresponding residue near the Q_i pocket of cytochrome *bc* complexes. The converse H217R mutation in the *bc* complex of *Rhodobacter capsulatus* increases the binding affinity of the Q_i semiquinone, increases the amplitude of *b* heme reduction, and slows electron transfer through the complex (33). We report here that the PetB R214H mutation in *Synechococcus* decreases the overall growth and cytochrome *bf* turnover rates, slows electron transfer across the membrane between the two *b* hemes, and thus defines a key residue for quinone-reductase (Q_i site) function in cytochrome *bf* complexes. These data are interpreted in light of the *bc* and *bf* structures, and a model is proposed for Q_i site catalysis in the cytochrome *bf* complex.

MATERIALS AND METHODS

Cyanobacterial Cultures—Stock cultures of *Synechococcus sp*. PCC 7002 were grown under cool white fluorescent lamps (20–30 μmol photons m^{-2} s^{-1}) in medium A as described previously (31). R214H mutant cultures were supplemented with streptomycin (Sm) and spectinomycin (Sp) at 50 μg/ml. For growth rate determinations, mid-log phase cells were inoculated into medium A (bubbled with 1% CO_2 in air) and incubated at 39 °C and 250 μmol photons m^{-2} s^{-1} light intensity. Cell density was determined by direct turbidity measurements on 18-mm-diameter culture tubes in a Spectronic 20D spectrophotometer (Milton Roy, Rochester, NY). Cultures for assays were grown at 200–250 μmol photons m^{-2} s^{-1} light intensity and harvested at mid-log phase. Chlorophyll concentrations were determined as described in Ref. 34. *Synechococcus* strain BstUI (31) is wild type for *petB* but carries the same Sm/Sp resistance cassette upstream of *petB* as in the R214H mutant. The BstUI strain was used as a control in some experiments. Its salient properties are indistinguishable from the wild type.

Site-directed Mutagenesis of the Synechococcus petB Gene—Escherichia coli strains were grown in LB medium supplemented as needed with 150 μg/ml of ampicillin, 15 μg/ml tetracycline, or 25 μg/ml each of Sm and Sp as described previously (31). Standard molecular genetic manipulations were performed as in (35). Plasmid pA6.2 carrying the *Synechococcus petBD* genes was used for site-directed mutagenesis of *petB* as described in Ref. 31. The *petB* R214H mutation was created by means of the mutagenic oligonucleotide 5′-CCACTTCCTCATG/ATtCaTAAGCAAGGTATTTC-3′. The lowercase letters identify the modified bases (wild type ATC CGT > ATt CaT in the R214H mutant), and the underlining indicates the newly created HinfI restriction site tag. The R214H mutation in plasmid pA6.2 was verified by plasmid isolation from *E. coli* transformants, PCR amplification from the primers TK-1 (5′-GACAGAGCAAGCTGTGTTAC-3′) or TL-F (5′-ACGATCACCGTTTCCTTC-3′) and TK-2 (5′-AGCCATCGCCACCGGACGAC-3′) (locations shown in Fig. 2), and restriction tests for the HinfI tag.

Plasmid pA6.2-R214H carrying the *petB* R214H mutation was introduced into *Synechococcus* by transformation (31). Because this plasmid cannot replicate in *Synechococcus*, selection for Sm/Sp resistance forces integration into the genome of the Sm/Sp resistance cassette and flanking *petBD* sequences as illustrated in Fig. 2. Integration of the *petB*-R214H mutation and segregational loss of the wild type *petB* allele were confirmed by: (i) PCR amplification of *petB* from *Synechococcus* transformants and restriction tests for the HinfI tag as described above for *E. coli*, (ii) allele-specific PCR detection of the *petB*-R214H allele according to Ref. 31 as shown in Fig. 2*B*, and (iii) DNA sequencing of *petB* PCR products from the TL-F and TK-2 primers. Forward primers for allele-specific PCR were 5′-CCACTTCCTCATGATCCG-3′ (for detection of wild type *petB*) or 5′-CCCACTTCCTCATGATtCa-3′ (for detection of

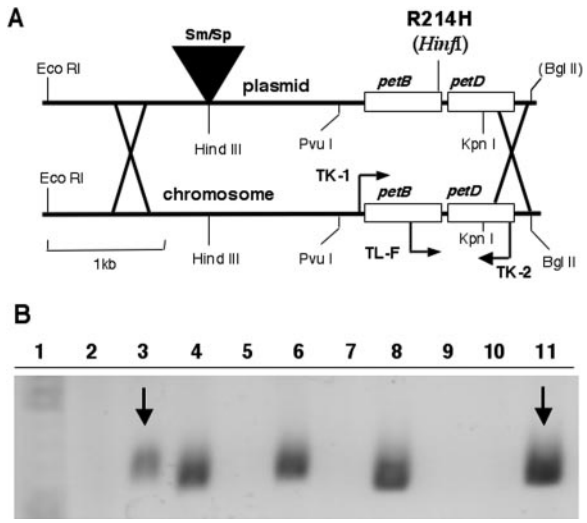

FIG. 2. **Strategy for site-directed mutagenesis and characterization of mutants by allele-specific PCR.** *A* illustrates the allele replacement strategy used to introduce mutant *petB* genes into the *Synechococcus* genome (31). Mutant *petB* alleles on a nonreplicating plasmid (*top line*) integrate into the genome via homologous recombination. Transformants are initially selected for Sm/Sp resistance. *B* shows allele-specific PCR tests of putative R214H transformants. *Lanes 2–11* show DNAs from transformants amplified from wild type (*lanes 2*, *4*, *6*, *8*, and *10*) and R214H mutant-allele detection primers (*lanes 3*, *5*, *7*, *9*, and *11*). Each pair of lanes (*lanes 2* and *3*; *lanes 4* and *5*; *lanes 6* and *7*; *lanes 8* and *9*; and *lanes 10* and *11*) contains one of five different DNA templates. The PCR product at 510 bp in *lanes 3* and *11* (marked by *arrows*) and its absence in *lanes 2* and *10* indicate that two of five transformants tested were segregants in which the *petB* R214H allele had replaced the wild type allele.

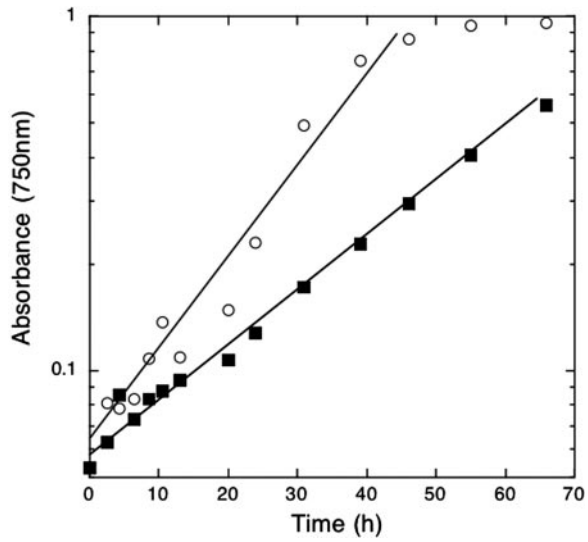

FIG. 3. **Growth of the *Synechococcus* R214H mutant.** The *petB* R214H mutant and control strain were grown at 250 μmol photons m^{-2} s^{-1} and 39 °C in A medium bubbled with 1% CO_2 in air. ○, BstUI control strain; ■, the R214H mutant. A linear curve fit was used for the exponential phase of growth. The BstUI strain is wild type for *petB* (cytochrome b_6).

the mutant *petB*-R214H allele). Both were used with the reverse primer, TK-2. DNA sequencing reactions were sent to the University of Wisconsin Madison Biotechnology Center for analysis.

Spectroscopic Measurements—Turnover of the cytochrome *bf* complex was monitored by measuring the rate of reduction of cytochrome f/c_6 following a saturating 40-ms light pulse as described previously (31, 34). Time-resolved absorbance changes were measured in the α-band region (530–570 nm) of the cytochromes. Because the spectra of cytochromes *f* and c_6 are largely superposed, and transfer between them is rapid, no effort was made to monitor these carriers separately (31). To improve the signal to noise ratio, the measurements were averaged with an interval between flashes of 7–10 s. The cells were suspended at 1–5 μM chlorophyll in reaction medium containing 5 mM Hepes, pH 7.5, 10 mM NaCl, and 10 mM $NaHCO_3$, at 39 °C. Prior to recording data, samples were light adapted by exposure to a series of saturating light flashes. The data shown are averages from three samples.

Single turnover experiments were performed at room temperature, using a "Joliot-type" spectrophotometer (36). Actinic flashes were provided by a xenon lamp (3 μs at half-height) filtered through a Schott filter (RG 695). Flashes were fired at a frequency of 0.15 Hz and were nonsaturating (hitting ~ 20% of the reaction centers) unless otherwise indicated. Cyanobacteria were kept in the dark under an argon atmosphere in a large reservoir, connected to the measuring cuvette, to ensure dark reduction of the plastoquinone pool. Cytochrome b_6 redox changes were evaluated as the difference between absorption at 563 nm and a base line drawn between 545 and 573 nm. At intervals following an actinic flash, the transmission of weak, monochromatic light passing through the sample was measured relative to a reference sample shielded from actinic light. Data were expressed as the difference (ΔI) in light transmission between the sample and reference cuvettes, normalized to light transmission (I) by the reference cuvette as in (36, 37). Cells were collected in the exponential phase of growth and resuspended in 20 mM Hepes buffer, pH 7.2, containing 20% Ficoll (w/v) to prevent cell sedimentation. 3-(3′,4′-Di-chloroprenyl)-1–1-dimethylurea and hydroxylamine were added at concentrations of 10 μM and 1 mM, respectively, to block photosystem II activity. Alternatively, the cells were harvested and resuspended in the same buffer containing D_2O (99.8% D atom) with a pellet/buffer volume ratio of 1/10 and stirred for 1 h. After a second centrifugation, the cell pellet was resuspended in the same buffer, with a pellet/buffer volume ratio of 1/20. No increase in the kinetic isotope effect was observed when the duration of the incubation in D_2O was increased.

Electrochemical Redox Titrations—Membranes of the *Synechococcus* R214H mutant were prepared and redox titrations performed in an electrochemical cell as described previously for wild type *Synechococcus* (38). The membrane pellet was resuspended in 50 mM MOPS, pH 7.0, 50 mM KCl buffer containing the redox mediators anthraquinone 2-sulfonate (−225 mV), anthraquinone 1,5-disulfonate (−170 mV), 2-hydroxy-1,4-naphthoquinone (−145 mV), anthraquinone (−100 mV), 2,5-dihydroxy-2-benzoquinone (−60 mV), menadione (0 mV), and 1,4-naphthoquinone (+60 mV), each at a concentration of 100 μM. Cytochrome b_6 absorbance spectra in the 540–580 nm range were recorded at ~25-mV intervals from samples poised at electrical potentials of −200 mV to +35 mV. The cytochrome b_6 peak absorbance values at 564 nm were plotted as a function of potential. The midpoint potentials of the b_6 hemes were calculated by fitting these data to a sum of two Nernst equations (each $n = 1$) as in previous analysis of wild type *Synechococccus* (38). Alternatively, a global fit analysis was performed as in Ref. 38, where the entire spectra were deconvoluted and fitted to a sum of Nernst curves. Both procedures yielded essentially identical results.

RESULTS

Construction of the PetB R214H Mutant and Characterization of Growth—As stated, both photosynthetic and respiratory electron transport in cyanobacteria require the cytochrome *bf* complex, and therefore essential subunits cannot be inactivated (reviewed by Ref. 5). Accordingly, the PetB R214H mutation was constructed by allele replacement (31). This method leaves a copy of the antibiotic resistance cassette upstream of the targeted gene in the *Synechococcus* genome as illustrated in Fig. 2*A*. The Sm/Sp cassette does not detectably alter the growth or electron transfer properties of control cells (31). *Synechococcus* R214H mutant segregants were confirmed as shown in Fig. 2*B* and detailed under "Materials and Methods."

Synechococcus mutant cells carrying the R214H mutation in the presumptive quinone-reductase site were initially characterized for growth properties and possible sensitivity to the cytochrome *bc* Q_i site inhibitor antimycin A. At 39 °C, 250 μmol photons m^{-2} s^{-1}, and 1% CO_2, the R214H mutant grew ~2.5-fold more slowly than the wild type. Fig. 3 shows a typical experiment. Specific growth rates and doubling times under these conditions were ~ 0.053 h^{-1} (doubling time, ~13 h) and ~0.19 h^{-1} (doubling time, ~3.5 h) for the mutant and control

cells, respectively. Under slower growth conditions (32 °C, 80 μmol photons m^{-2} s^{-1}, and atmospheric CO_2), mutant and control cells grew at similar rates. Mutant and control cultures were insensitive to antimycin (30 μM) under all conditions (not shown). These data indicate that the R214H mutation did not alter the antimycin insensitivity of the cytochrome *bf* Q_i site but did suggest a partial blockage of electron flow to this site resulting in slower growth under conditions of high electron flux.

Turnover of Cytochrome bf Complexes in Wild Type and R214H Mutant Cells—Plastoquinol oxidation in the cytochrome *bf* complex operates via a branched pathway, where one electron is transferred to the high potential chain and the second electron is transferred to the low potential chain (Fig. 1). The overall rate of electron flow through the complex can therefore be evaluated by measuring the rate of cytochrome *f*/c_6 rereduction (the spectra of the two redox partners are largely superposed) after a long flash (31). The rationale for this measurement is that light induces the oxidation of the redox cofactors (the P700 reaction center of photosystem I, cytochromes *f* and c_6, and the Rieske ISP 2Fe-2S cluster) that are functionally located downstream of the rate-limiting, plastoquinol oxidation step. When the light is turned off, plastoquinol oxidation drives the reduction of the ISP cluster, cytochromes *f* and c_6, and P700. This process is proportional to the rate of plastoquinol oxidation but is also indicative of the overall turnover of the *bf* complex. If the Q cycle is continuously engaged during cytochrome *bf* turnover, as proposed (39), then the cytochrome *f*/c_6 rereduction rate also depends on the Q_i site reduction of plastoquinone. The complex has to perform several turnovers to generate all of the reducing equivalents required to reduce the pool of electron carriers in the high potential chain (31, 38).

We employed this technique as a first approach to gain information on the turnover efficiency of the cytochrome complex in the R214H mutant cells. Fig. 4*A* presents the absorbance changes from 540 to 570 nm measured in intact wild type and mutant cells following a 40-ms flash. Here reduction and oxidation processes are shown as increases or decreases in absorbance, respectively. The spectra show that the absorbance change following illumination is made up of contributions from cytochrome *f* (α-band maximum 556 nm in *Synechococcus* sp. PCC 7002, Ref. 38) and cytochrome c_6 (α-band maximum 553 nm in *Synechococcus*, Ref. 38) in both strains.

Fig. 4*B* presents a typical experiment where the kinetics of electron flow in cytochrome *f*/c_6 were estimated in both the wild type and mutants strains. In the absence of inhibitors, the half-times of cytochrome *f*/c_6 reduction were 18 ± 1 ms in the wild type, in substantial agreement with previous estimates (31), and 46 ± 2 ms in the R214H mutant, indicating a significant decrease in cytochrome *bf* turnover efficiency. These values did not change upon the addition of antimycin A (data not shown) indicating, as in the growth experiments, that the simple replacement of cytochrome b_6 Arg^{214} with histidine did not confer specific antimycin binding and inhibitor sensitivity.

Single Turnover Flash-induced Cytochrome b_6 Redox Changes—Having demonstrated that the overall turnover of the cytochrome *bf* complex was slowed in the R214H mutant, we tried to gain more direct information on the specific reaction step affected. To this end, we studied flash-induced, single-turnover absorption changes associated with redox events in the b_6 hemes. These reactions are indicative of electron transfer processes that occur both at the Q_o (cytochrome b_6 reduction) and Q_i (cytochrome b_6 oxidation) sites. The experiments were performed with intact cells, as described previously (38). The results of such measurements are presented in Fig. 5.

Fig. 5 (*A* and *B*) shows flash-induced absorbance changes

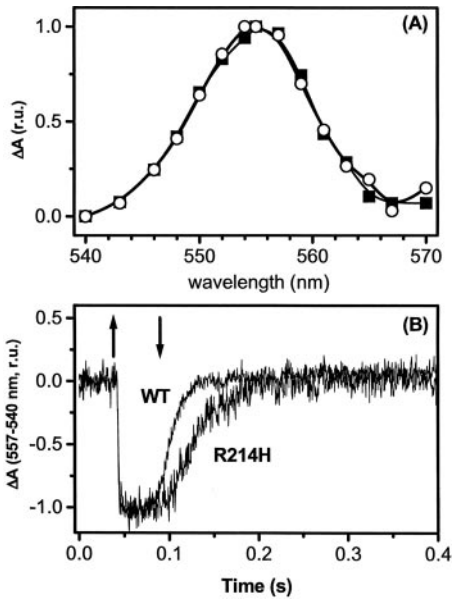

FIG. 4. **Spectra of light-induced absorbance changes in the cytochrome *f*/c_6 spectral region and cytochrome *f*/c_6 oxidation-reduction kinetics.** *A*, spectra of absorbance changes in *Synechococcus* cells following a 40-ms saturating flash. BstUI control (■) and R214H mutant cells (○) were suspended in 5 mM Hepes, pH 7.5, 10 mM NaCl, 10 mM $NaHCO_3$ at chlorophyll concentrations of 4.20 and 1.51 μM, respectively. Further details are given in the text. *B*, cytochrome *bf* turnover as measured by cytochrome *f*/c_6 rereduction. Saturating actinic light (40 ms) was turned on and off as indicated by the *arrows*. Intact BstUI control (*WT*) and R214H mutant cells were suspended as in *A*. The flash-induced absorbance changes at 557 minus 540 nm reflect the oxidation and reduction of cytochromes *f* and c_6. The spectra were normalized to equivalent maximum absorbance changes.

recorded in the 550–580-nm region, in the presence of FCCP (*solid squares*) or FCCP and NQNO (*open squares*). Data from both the wild type (Fig. 5*A*) and R214H mutant (Fig. 5*B*) revealed spectra with absorbance maxima at ~563 nm, typical of cytochromes b_6 (38). The difference between absorbance at 563 nm and a base line drawn between 545 and 573 nm was subsequently monitored to track the b_6 heme reduction and oxidation kinetics shown in Fig. 5, *C* and *D*. In wild type cells (Fig. 5*C*), illumination resulted in the appearance of a small signal increase (reflecting cytochrome b_L reduction), followed by a large signal decrease. The latter is attributable to oxidation of the b_H heme at the Q_i site. Indeed, no redox signal changes are expected during electron transfer between the b_L and b_H hemes, because their spectra *in vivo* are almost identical (Refs. 11, 38, and 40 and references therein). Upon the addition of the Q_i site inhibitor, NQNO (29), the cytochrome b_6 oxidation kinetics were slowed considerably, whereas the reduction process remained largely unaffected (compare the initial positive slopes). Consequently, the amplitude of the reduction phase increased at the expense of the oxidation signal, and the rate of electron injection into the low potential (cytochrome b_L and b_H) chain could be correctly estimated.

From these single-turnover data, we estimated a $t_{1/2}$ for cytochrome b_6 reduction in the 2-ms range in agreement with a previous estimation based on the deconvolution of time-resolved spectra (38). Note that because of the bifurcated reaction mechanism at the Q_o site, electron transfers to the high (cytochrome *f*/c_6) and low (b_6 heme) potential branches are expected to occur at similar rates as confirmed here (not shown) and demonstrated previously for *Synechococcus* 7002 (38). The almost 1-order of magnitude difference between our single-flash estimation of Q_o site turnover based on b_6 heme reduction and that obtained from cytochrome *f*/c_6 reduction after long flash

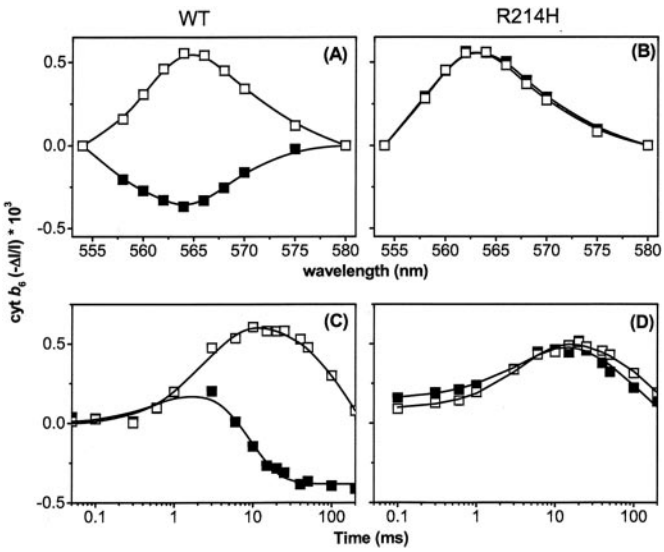

FIG. 5. **Light-induced redox changes in the 555–580-nm spectral region measured upon single turnover flash illumination (*A* and *B*) and kinetics of cytochrome b_6 redox changes (*C* and *D*).** Cells were collected during exponential growth and resuspended in Hepes 20 mM pH 7.2, with the addition of 20% (w/v) Ficoll to prevent sedimentation. The cells were illuminated with red flashes at a frequency of 0.15 Hz. 3-(3′,4′-Di-chloroprenyl)-1–1-dimethylurea and hydroxylamine were added at concentrations of 10 μM and 1 mM, respectively, to block photosystem II activity. The ionophore FCCP (1 μM) was added to remove the electrochemical proton gradient and its effects of the rate of plastoquinone reduction at the Q_i site. Data shown are from cells in the absence (■) and presence (□) of the Q_i site inhibitor NQNO at 4 μM. *A* (wild type, *WT*) and *B* (R214H mutant). The spectra were recorded 40 ms after the actinic flash illumination and normalized at their extremes to correct for the contribution of cytochrome f/c_6 absorption. By this time, however, the cytochromes f/c_6 were largely rereduced, and their contribution to the overall absorption did not exceed 10%. *C* (wild type) and *D* (R214H mutant) kinetics. Flash intensity was 20% of the saturating value to prevent multiple turnovers of the electron transfer chain. $\Delta I/I$ is the difference (ΔI) in light transmission between the sample and reference cuvettes, normalized to light transmission (I) by the reference cuvette.

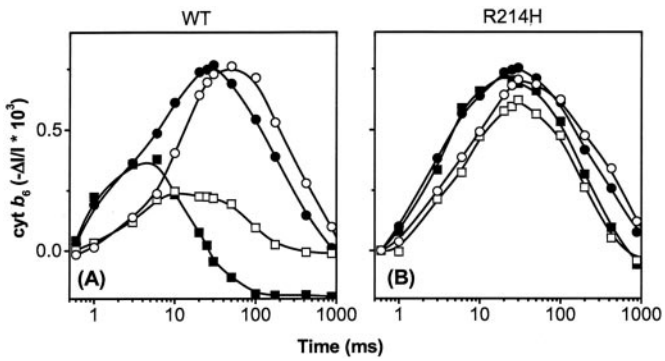

FIG. 6. **Kinetic isotope effects on cytochrome b_6 redox changes.** Experimental conditions were the same as those described in the legend of Fig. 5, except that measurements were performed in the presence of H_2O or D_2O as detailed under "Materials and Methods." FCCP was present at 1 μM to prevent build-up of the electrochemical proton gradient. Data shown are from cells in H_2O (■), D_2O (□), H_2O with 4 μM NQNO (●), and D_2O with 4 μM NQNO (○). *WT*, wild type.

illumination (Fig. 4) can be explained by the occurrence of multiple turnovers in the latter as stated above.

The R214H mutant cells displayed rather different kinetics as shown in Fig. 5*D*. Here, the traces recorded in the absence and presence of NQNO were largely superposed. In the mutant, the rate of cytochrome b_6 reduction (which represents the oxidation of the plastoquinol pool at the Q_o site) was substantially unaffected, but the oxidation of the b_6 hemes was greatly slowed ($t_{1/2}$ = ~80 ms relative to ~8 ms in the wild type). In sharp contrast to the wild type, the addition of the Q_i site inhibitor did not further slow *b* heme oxidation in the R214H mutant. This clearly suggests that the turnover of the Q_i site was specifically altered by the mutation, in agreement with our expectations.

Isotopic Effect on Cytochrome b_6 Oxidation Kinetics—In green algae, the substitution of D_2O for H_2O influences the kinetics of cytochrome *bf* electron transfer reactions. In particular, this effect mostly concerns the reactions that follow plastoquinol oxidation at the Q_o site (41) and plastoquinone reduction (or cytochrome b_6 oxidation) at the Q_i site (37). The interpretation for this isotopic effect is that deprotonation and protonation of the quinones kinetically limits the reactions occurring in both the Q_o and Q_i sites.

To investigate whether the slow-down of cytochrome b_6 oxidation in the R214H mutant resulted from a decreased efficiency of electron transfer or a modification of the protonation process, we measured b_6 heme kinetics in cyanobacteria following H_2O-D_2O exchange according to procedures developed for *C. reinhardtii* (see "Materials and Methods"). With the wild type, we obtained results closely resembling those previously reported for *C. reinhardtii* (37). Both the reduction and oxidation rates of the cytochrome b_6 hemes decreased substantially in D_2O-enriched medium (compare the *solid* and *open squares* in Fig. 6*A*), consistent with the direct involvement of proton transfer events in these reactions. The isotopic effect on cytochrome b_6 oxidation was largely decreased by pretreatment with the Q_i site inhibitor NQNO, suggesting that under these conditions, processes other than protonation of the Q_i plastoquinone (for example, its binding to the Q_i site or its reduction by the b_H heme) limited the turnover of the Q_i site.

In the R214H mutant, only a very small isotopic effect was observed on the cytochrome b_6 oxidation kinetics, independent of the presence of NQNO (Fig. 6*B*). This indicates that electron transfer reactions limited quinone reduction in the mutant and further supports the conclusion that the R214H mutation mimics the effect of NQNO.

Evaluation of the Cytochrome b_6 Redox Potentials in the R214H Mutant—Our data suggested that the kinetic consequences of the R214H mutation could be attributed either to a change in the redox potential of the Q_i hemes (hemes b_H and/or heme c_i (*x*)) or to a decreased affinity of plastoquinone for its Q_i-binding site. To determine whether the redox potential of the b_H heme was modified in the mutant, we performed an equilibrium redox titration of membranes extracted from the R214H mutant. In the −200 to +35 mV range, two components were clearly identified that had equivalent absorption spectra characteristic of cytochromes b_6 (Fig. 7). Their redox potentials were indistinguishable within experimental error from those previously determined for the wild type (38). We ruled out, therefore, that a modification of the b_H heme redox potential was responsible for the kinetic effects observed in the R214H mutant.

In the spectral region analyzed, no evidence was found for a third redox component. This indicates that the c_i (*x*) heme of the Q_i domain was silent in the α band region, consistent with its expected high spin nature (9, 10). Because of strong chlorophyll absorbance, we were unable to perform redox titrations of membranes in the Soret region and therefore could not assess the redox properties of the c_i (*x*) heme.

DISCUSSION

Functional Phenotype of the R214H Mutant—We have shown here that replacement of the conserved Arg^{214} with histidine in cytochrome b_6 dramatically impairs Q_i site function, turnover of the cytochrome *bf* complex, and the growth of *Synechococcus*

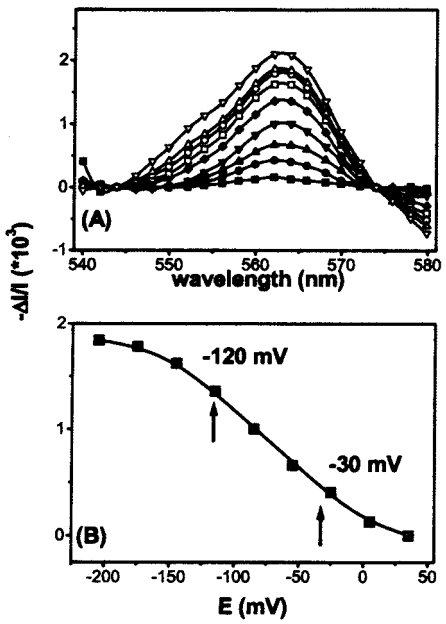

FIG. 7. **Redox titration of membranes isolated from the R214H mutant.** Titrations were performed in 50 mM MOPS, pH 7.0, 50 mM KCl buffer in the −200 mV to +35 mV range as described under "Materials and Methods." *A* shows spectra obtained in the cytochrome b_6 spectral region from membranes poised at the potentials listed below. *B* shows the peak absorbance values for cytochrome b_6 (at 564 nm) as a function of the applied potential. The midpoint potentials of the two b_6 hemes were calculated either by fitting the data in *B* to the sum of two $n = 1$ Nernst equations or by globally fitting the spectra in *A* to Nernst equations as described under "Materials and Methods." The two procedures gave similar results. The absorbance changes are expressed as $\Delta I/I$ as in Fig. 5. ▽, −200 mV; △, −175 mV; ○, −145 mV; □, −115 mV; ♦, −85 mV; ▼, −55 mV; ▲, −25 mV; ●, 5 mV; ■, 35 mV.

cells. As mentioned, the cytochrome *bf* Q_i site and transmembrane electron transfer between the b_6 hemes have been enigmatic and difficult to study. Principally (i) there is no highly efficient inhibitor such as antimycin A to block electron transfer at the cytochrome *bf* Q_i site (16), (ii) no stable Q_i-semiquinone and accompanying EPR signal have been detected (16), and (iii) the spectral properties of the b_H and b_L hemes are virtually identical within intact cells (38, 40, 42). All of these factors have made it exceedingly challenging to track individual redox changes within the low potential chain. As a consequence, there has been much controversy about the role of the Q_i site for cytochrome *bf* turnover and whether the Q cycle mechanism of electron transfer (described above) operates requisitely or facultatively (see Refs. 5, 11, 43, and 44 for reviews). Several interesting alternative mechanisms for electron and proton transfer have been proposed that might operate in *bf* complexes under particular environmental conditions. These include "semiquinone" (36), "proton pump" (45–47), and "bypass" (43) models that involve transfer of semiquinones or protons across the membrane or the transfer of two electrons from plastoquinol to two Rieske ISP clusters in a cytochrome *bf* dimer on the lumenal side of the membrane. Most of these mechanisms still require the operation of a quinone-reductase (Q_i) site, in some form, on the electronegative side of the membrane.

To help elucidate Q_i site function in the cytochrome *bf* complex, we attempted to make the cytochrome *bf* complex of the cyanobacterium *Synechococcus* 7002 more like the *bc* complex. Because this project was initiated before the recent cyanobacterial (9) and algal (10) cytochrome *bf* structures, the rationale employed to design the mutation was based on homology to the cytochrome *b* protein of *R. capsulatus* (33). Cytochrome b_6 Arg^{214} of *Synechococcus* corresponds to the conserved cytochrome *b* His^{217} of *R. capsulatus* (and to cytochrome *b* His^{202} of yeast shown in Fig. 8, *right panel*). The H217R mutation of *R. capsulatus* greatly increased (by ~10-fold) the binding affinity of semiquinone for the Q_i site and thereby slowed Q_i site turnover, increased the reduction level of heme b_H, and slowed overall turnover of the *bc* complex.

Our corresponding R214H mutation in *Synechococcus* did not generate an antimycin-sensitive cytochrome *bf* complex, nor did it alter the spectra of the b_6 hemes, but it did markedly alter Q_i site catalysis and the overall turnover of the cytochrome *bf* complex. In the cytochrome *bf* structures (9, 10), Arg^{214} (equivalent to Arg^{207} in both *Mastigocladus* and *Chlamydomonas*) lies within or close to the Q_i pocket and the newly discovered c_i (*x*) heme (Fig. 8, *left* and *middle panels*). Therefore, the removal of this positively charged residue might not only alter the affinity of the Q_i site for plastoquinone but also the midpoint potentials of the redox cofactors within its vicinity. Our redox titration of the *b* hemes from the R214H mutant revealed midpoint potentials similar, within experimental error, to those from wild type *Synechococcus*. This seemed surprising in light of the relatively close proximity of Arg^{207} (*Synechococcus* Arg^{214}) to the b_H heme and the likely electronic coupling of the b_H and c_i (or *x*) hemes via a heme b_H propionate and a water molecule in both the *Mastigocladus* and *Chlamydomonas* structures (9, 10). If the Q_i site structure is more like that in Fig. 8 (*left panel*), then the interaction of the c_i (*x*) heme propionates with Arg^{207} (*Synechococcus* Arg^{214}) should modulate the positive charge of the arginine, and there might be less direct influence on heme b_H. Similarly, if Arg^{207} (*Synechococcus* Arg^{214}) has a direct role in binding plastoquinone, again as suggested in Fig. 8 (*left panel*), the effect of the R214H mutation on heme b_H might be minimized. For these reasons, we believe that our data favor a direct role for Arg^{207} (*Synechococcus* Arg^{214}) in plastoquinone binding at the Q_i site, although we cannot exclude other possibilities. We were unable to directly assess the midpoint potential of the c_i (*x*) heme in the mutant because of the absence of either a distinguishing optical signal, as discussed above, or a well defined EPR signal.

Thanks to its unique position in the structure, Arg^{207} (*Synechococcus* Arg^{214}) may have additional roles in Q_i site catalysis. Besides plastoquinone binding and stabilization of a negative charge on heme c_i (*x*) (see below), it may participate in proton transfer to the Q_i quinone, either by providing a direct path for protons or indirectly by participating in a network of residues involved in protonation. Such protonation networks are well established in the Q_B pocket of the bacterial reaction center (48, 49). In the cytochrome *bf* structures, Arg^{207} (*Synechococcus* Arg^{214}) may be hydrogen-bonded to plastoquinone via a water molecule. As detailed by Kurisu *et al.* (9) and Stroebel *et al.* (10), heme c_i (*x*), and the Q_i pocket are relatively accessible to the stromal, aqueous phase being bounded mostly by the N- and C-terminal loops of cytochrome b_6 and the N-terminal extension of subunit IV. Thus, Arg^{214} could be a link in a short water chain such as that in cytochrome *bc* Q_i (50–52) or the reaction center Q_B sites (49, 53).

Our data showed a considerable kinetic isotope effect on both the reduction and oxidation kinetics of the b_6 hemes in wild type *Synechococcus* cells (Fig. 6). This implies that steps in both plastoquinol deprotonation at the Q_o site and plastoquinone protonation at the Q_i site affect the overall reactions at these sites as shown previously for chloroplasts (37, 54). The R214H mutant showed a small isotope effect on b_6 heme reduction but virtually none on b_6 heme oxidation, indicating that an electron transfer step has been slowed at least as much as any of the protonation steps. These data do not preclude a role for Arg^{214}

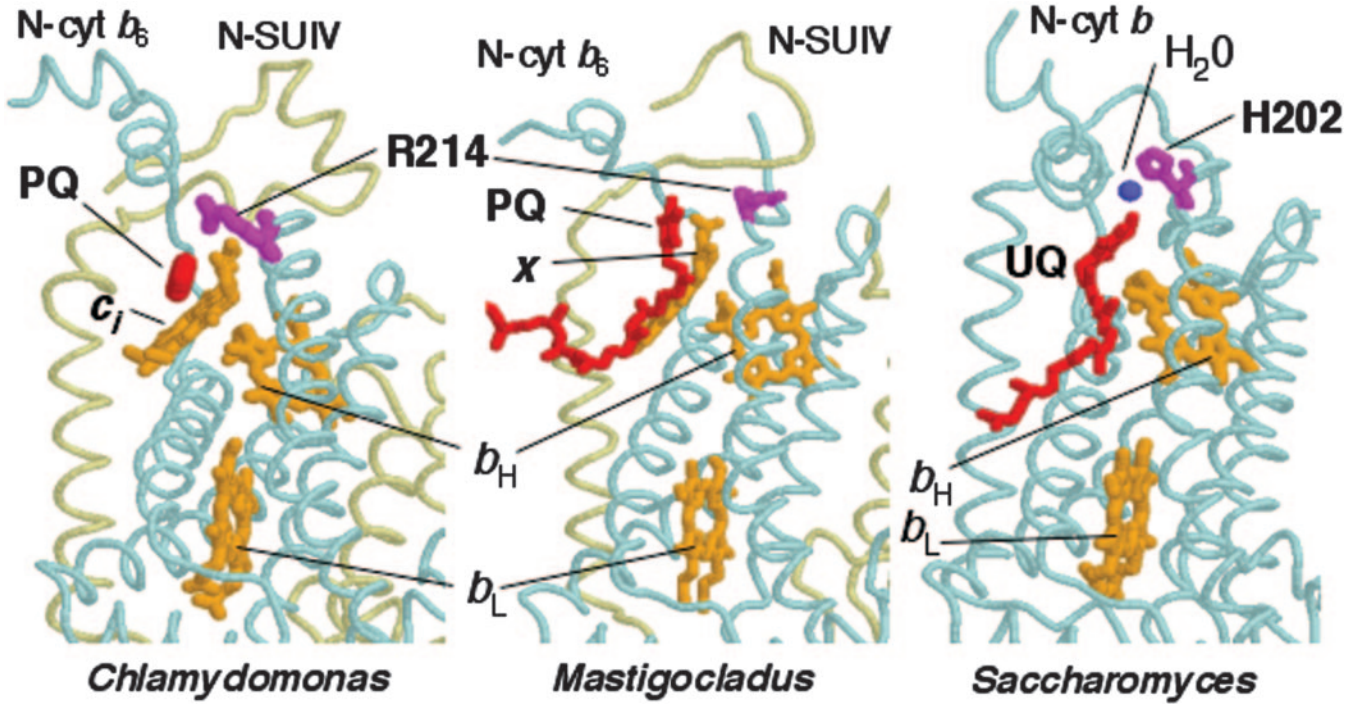

FIG. 8. **Quinone reductase domains of the *Chlamydomonas* and *Mastigocladus* cytochrome *bf* complexes and the yeast mitochondrial cytochrome *bc* complex.** Backbone traces of the cytochrome b_6 or yeast cytochrome *b* (*light cyan*) and subunit IV (*light yellow*) polypeptides are shown together with the b_L, b_H, and c_i hemes (*orange*). Yeast ubiquinone (*UQ*), *Mastigocladus* plastoquinone (*PQ*), and the plastoquinone ring in the *Chlamydomonas* structure are in *red*. Arg^{214} (equivalent to *Chlamydomonas* or *Mastigocladus* Arg^{207}) and the corresponding His^{202} in yeast are *magenta*. A water molecule between His - and ubiquinone in the yeast Q_i site is *blue*. Coordinates from the *Chlamydomonas* (10) and *Mastigocladus* (9) cytochrome *bf* and the yeast (56) cytochrome *bc* structures were manipulated and displayed with the aid of the Swiss-Pdb Viewer (us.expasy.org/spdbv/) and Protein Explorer (molvis.sdsc.edu/protexpl/) programs.

in Q_i plastoquinone protonation in the native cytochrome *bf* complex.

Based on our findings, the main role of cytochrome b_6 Arg^{214} (Arg^{207} in the cytochrome *bf* structures) seems to be in modulating the binding affinity of the Q_i site for its plastoquinone substrate. In this sense, the R214H mutation of *Synechococcus*, which appears to weaken quinone binding, is indeed complementary to H217R of *R. capsulatus* where arginine at position 217 binds quinone more strongly than the native histidine.

Structural Features of Cytochrome b_6 Arg^{214}—Based on their characterization of the mutant phenotype, Gray *et al.* (33) proposed that His^{217} binds quinone at the cytochrome *bc* Q_i site in *R. capsulatus* via a hydrogen bond to one of the quinone carbonyls analogous to the interaction of a histidine with Q_B in the bacterial reaction center (55). Indeed, this predicted role of His^{217} has been largely confirmed by the structures of mitochondrial cytochrome *bc* complexes (17–20, 56). However, it remains controversial whether His^{217} (or the equivalent histidine in other *bc* complexes) directly participates in binding forms of the Q_i-quinone or does so via a linking water molecule. Some cytochrome *bc* structures (18, 57) and EPR investigations (52, 57) support the former, whereas others (51, 56), where the distance between this histidine and quinone is too great for hydrogen bonding, favor the latter. These structural differences may reflect dynamic, functional aspects of cytochrome *bc* Q_i domains as proposed in recent models of ubiquinone reduction and protonation (51, 52, 57). Fig. 8 (*right panel*) illustrates the juxtaposition of His^{202} (equivalent to *R capsulatus* His^{217}) and ubiquinone via hydrogen-bonds to a linking water molecule in the Q_i pocket of the yeast cytochrome *bc* structure (56).

There are clear differences among the three Q_i site structures shown in Fig. 8. In the *Chlamydomonas* structure, Arg^{207} (*Synechococcus* Arg^{214}) lies close to the c_i heme (Fig. 8, *left panel*). One of the arginine amino nitrogens is within easy hydrogen bonding distance of a c_i heme propionate oxygen. The Q_i site plastoquinone has not been unambiguously identified in the *Chlamydomonas bf* structure, but the quinone ring likely resides near the face of heme c_i (10).[2] This is represented by a *red ring* (viewed largely edge-on) in Fig. 8 (*left panel*). Because the quinone oxygens have not been assigned, likely hydrogen bonding interactions cannot be precisely deduced from the structure. However, depending on the orientation of these oxygens, the Arg^{207} (*Synechococcus* Arg^{214}) amino nitrogens could either be within direct, 3 Å, hydrogen bonding distance of the Q_i plastoquinone (as illustrated in Fig. 8, *left panel*) or be linked via an intervening water molecule as in the His^{202}-ubiquinone linkage in the yeast Q_i site (Fig. 8, *right panel*, and Ref. 50).

In the *Mastigocladus* structure, the Arg^{207} amines face away from heme *x* (c_i) and the assigned location of the Q_i plastoquinone (Fig. 8, *middle panel*). In this position, direct hydrogen bonding to plastoquinone or heme *x* is not possible. The shortest distance from the arginine nitrogens to heme *x* propionates is ~8 Å, and the distance to the heme b_H propionates is slightly greater. In this conformation, an interaction of Arg^{207} via an intervening water molecule or that of a different rotamer of the arginine with heme *x* might still be possible.

The observed structural differences of the cytochrome *bf* Q_i domains may reflect: (i) evolutionary and functional differences between chloroplast and cyanobacterial cytochrome complexes; (ii) interesting conformational changes that occur during Q_i site catalysis, as in the Q_B sites of reaction centers (58), the quinol-oxidase (Q_o) domains of *bc* complexes (12), and those postulated for *bc* Q_i domains (51, 52, 57); or (iii) artifacts resulting from local differences in resolution and interpretation

[2] D. Picot, personal communication.

of electron densities. The phenotype observed here is more consistent with the description of the Q_i site obtained from *Chlamydomonas*. Nevertheless, our data cannot rule out other possible interpretations such as a very tight interaction of Arg^{214} with the c_i (*x*) heme. Further analysis will be needed to resolve this question.

Electron Flow through Inhibited Q_i Sites in Cytochrome bf Complexes—We have shown that the *Synechococcus* R214H mutation had an effect like that of NQNO, which slows b_6 heme oxidation and partially slows the turnover of the cytochrome *bf* complex (29). Surprisingly, the addition of NQNO to the R214H mutant did not further slow the *b* heme oxidation kinetics (Fig. 6*B*). This could imply that Arg^{214} provides a crucial binding site for NQNO and that the inhibitor binds poorly to the mutant complexes. Alternatively, electron transfer from heme b_H to the Q_i plastoquinone might already be largely (or perhaps completely) blocked either in the R214H mutant or by NQNO at 4 μM. The addition of NQNO to the mutant would then have no further impact. Turnover of the cytochrome complex under these conditions (~30% that of the wild type) could only occur if there were a bypass or "electron leak" pathway that allows electrons to be diverted from Q_i plastoquinone reduction.

The cytochrome *bf* structures reveal accessibility of the c_i (*x*) heme to the stromal compartment, raising the possibility of Q_i site access to ferredoxin or ferredoxin NAD(P)H oxidoreductase in a cyclic electron pathway around photosystem I (9, 10, 59). This being the case, the slow electron leak observed here might not reflect inefficient plastoquinone reduction in poorly inhibited Q_i sites but perhaps a type of "reverse cyclic" pathway where electrons from heme c_i (*x*) (or a modified lower potential heme c_i or *x*) could reduce ferredoxin NAD(P)H oxidoreductase or ferredoxin. In recent work, Osyczka *et al.* (15) have discussed how electron transfer in the *bc* complex might operate in reverse depending on equilibrium midpoint potentials and sizes of electron pools as documented, for example, in the "reverse," uphill electron transfer through the *bc* complex of *Thiobacillus ferrooxidans* (60).

Conclusion—Accumulating evidence indicates that under typical conditions in wild type organisms, electron transfer to the cytochrome *bf* Q_i site should proceed from heme b_L > heme b_H > heme c_i (*x*) > Q_i plastoquinone. As mentioned, the cytochrome *bf* structures present compelling evidence for electronic coupling of hemes b_L and c_i (*x*). It seems unlikely that the c_i (*x*) heme placement evolved for uniquely structural rather than functional reasons. We suggest that *Synechococcus* cytochrome b_6 Arg^{214} (*Mastigocladus* or *Chlamydomonas* Arg^{207}) plays a central role in Q_i plastoquinone binding. Moreover, data presented here demonstrate for the first time, that modification of the Q_i site of the cytochrome *bf* complex dramatically alters overall photosynthetic efficiency. This finding supports previous indications that the quinone-reductase reaction is continuously engaged during steady state photosynthesis (39), thus modulating H^+/e^- stoichiometries and efficient photosynthetic CO_2 assimilation.

Acknowledgment—We thank Daniel Picot for stimulating discussions and for the coordinates of the Q_i site plastoquinone ring in the *Chlamydomonas* cytochrome *bf* structure.

REFERENCES

1. Lemaire, C., Girard-Bascou, J., Wollman, F.-A., and Bennoun, P. (1986) *Biochim. Biophys. Acta* **851,** 229–238
2. Pierre, Y., Breyton, C., Kramer, D., and Popot, J. L. (1995) *J. Biol. Chem.* **270,** 29342–29349
3. Widger, W. R., Cramer, W. A., Herrmann, R. G., and Trebst, A. (1984) *Proc. Natl. Acad. Sci. U. S. A.* **81,** 674–678
4. Nitschke, W., Joliot, P., Liebl, U., Rutherford, A. W., Hauska, G., Muller, A., and Riedel, A. (1992) *Biochim. Biophys. Acta* **1102,** 266–268
5. Kallas, T. (1994) in *The Molecular Biology of the Cyanobacteria* (Bryant, D. A., ed) pp. 259–317, Kluwer Academic Publishers, Dordrecht, The Netherlands
6. Hauska, G., Schütz, M., and Büttner, M. (1996) in *Oxygenic Photosynthesis: The Light Reactions* (Ort, D. R., and Yocum, C. Y., eds) Kluwer Academic Publishers, Dordrecht, The Netherlands
7. Hamel, P., Olive, J., Pierre, Y., Wollman, F. A., and de Vitry, C. (2000) *J. Biol. Chem.* **275,** 17072–17079
8. Zito, F., Vinh, J., Popot, J. L., and Finazzi, G. (2002) *J. Biol. Chem.* **277,** 12446–12455
9. Kurisu, G., Zhang, H., Smith, J. L., and Cramer, W. A. (2003) *Science* **302,** 1009–1014
10. Stroebel, D., Choquet, Y., Popot, J. L., and Picot, D. (2003) *Nature* **426,** 413–418
11. Cramer, W. A., Soriano, G. M., Ponomarev, M., Huang, D., Zhang, H., Martinez, S. E., and Smith, J. L. (1996) *Annu. Rev. Plant Physiol. Plant Mol. Biol.* **47,** 477–508
12. Berry, E. A., Guergova-Kuras, M., Huang, L. S., and Crofts, A. R. (2000) *Annu. Rev. Biochem.* **69,** 1005–1075
13. Mitchell, P. (1976) *J. Theor. Biol.* **62,** 327–367
14. Crofts, A. R., Meinhardt, S. W., Jones, K. R., and Snozzi, M. (1983) *Biochim. Biophys. Acta* **723,** 202–218
15. Osyczka, A., Moser, C. C., Daldal, F., and Dutton, P. L. (2004) *Nature* **427,** 607–612
16. Hope, A. B. (1993) *Biochim. Biophys. Acta* **1143,** 1–22
17. Xia, D., Yu, C.-A., Kim, H., Xia, J.-Z., Kachurin, A. M., Zhang, L., Yu, L., and Deisenhofer, J. (1997) *Science* **277,** 60–66
18. Zhang, Z., Huang, L., Shulmeister, V. M., Chi, Y. I., Kim, K. K., Hung, L. W., Crofts, A. R., Berry, E. A., and Kim, S. H. (1998) *Nature* **392,** 677–684
19. Iwata, S., Lee, J. W., Okada, K., Lee, J. K., Iwata, M., Rasmussen, B., Link, T. A., Ramaswamy, S., and Jap, B. K. (1998) *Science* **281,** 64–71
20. Kim, H., Xia, D., Yu, C. A., Xia, J. Z., Kachurin, A. M., Zhang, L., Yu, L., and Deisenhofer, J. (1998) *Proc. Natl. Acad. Sci. U. S. A.* **95,** 8026–8033
21. Breyton, C. (2000) *Biochim. Biophys. Acta* **1459,** 467–474
22. Brugna, M., Rodgers, S., Schricker, A., Montoya, G., Kazmeier, M., Nitschke, W., and Sinning, I. (2000) *Proc. Natl. Acad. Sci. U. S. A.* **97,** 2069–2074
23. Breyton, C. (2000) *J. Biol. Chem.* **275,** 13195–13201
24. Witt, H. T. (1979) *Biochim. Biophys. Acta* **503,** 355–427
25. Crofts, A. R., and Wraight, C. (1983) *Biochim. Biophys. Acta* **726,** 149–185
26. Degli Esposti, M., de Vries, S., Crimi, M., Ghelli, A., Patarnello, T., and Meyer, A. (1993) *Biochim. Biophys. Acta* **1143,** 243–271
27. Dutton, P. L., and Jackson, J. B. (1972) *Eur. J. Biochem.* **30,** 495–510
28. Frank, K., and Trebst, A. (1995) *Photochem. Photobiol.* **61,** 2–9
29. Jones, R. W., and Whitmarsh, J. (1988) *Biochim. Biophys. Acta* **933,** 258–268
30. Joliot, P., and Joliot, A. (1986) *Biochim. Biophys. Acta* **849,** 211–222
31. Lee, T., Metzger, S. U., Cho, Y. S., Whitmarsh, J., and Kallas, T. (2001) *Biochim. Biophys. Acta* **1504,** 235–247
32. Yan, J., and Cramer, W. A. (2003) *J. Biol. Chem.* **278,** 20925–20933
33. Gray, K. A., Dutton, P. L., and Daldal, F. (1994) *Biochemistry* **33,** 723–733
34. Zhang, L., Pakrasi, H. B., and Whitmarsh, J. (1994) *J. Biol. Chem.* **269,** 5036–5042
35. Sambrook, J., Fritsch, E. F., and Maniatis, T. (1989) *Molecular Cloning: A Laboratory Manual*, Cold Spring Harbor Laboratory, Cold Spring Harbor, NY
36. Joliot, P., and Joliot, A. (1994) *Proc. Natl. Acad. Sci. U. S. A.* **91,** 1034–1038
37. Barbagallo, R. P., Breyton, C., and Finazzi, G. (2000) *J. Biol. Chem.* **275,** 26121–26127
38. Baymann, F., Rappaport, F., Joliot, P., and Kallas, T. (2001) *Biochemistry* **40,** 10570–10577
39. Sacksteder, C. A., Kanazawa, A., Jacoby, M. E., and Kramer, D. M. (2000) *Proc. Natl. Acad. Sci. U. S. A.* **97,** 14283–14288
40. Kramer, D. M., and Crofts, A. R. (1994) *Biochim. Biophys. Acta* **1184,** 193–201
41. Deniau, C., and Rappaport, F. (2000) *Biochemistry* **39,** 3304–3310
42. Furbacher, P. N., Girvin, M. E., and Cramer, W. A. (1989) *Biochemistry* **28,** 8990–8998
43. Cramer, W. A., Black, M. T., Widger, W. R., and Girvin, M. E. (1987) in *The Light Reactions* (Barber, J., ed) pp. 447–493, Elsevier Science Publishing Co., Inc., New York
44. Soriano, G. M., Ponamarev, M. V., Carrell, C. J., Xia, D., Smith, J. L., and Cramer, W. A. (1999) *J. Bioenerg. Biomembr.* **31,** 201–213
45. Joliot, P., and Joliot, A. (1998) *Biochemistry* **37,** 10404–10410
46. Joliot, P., and Joliot, A. (2001) *Biochim. Biophys. Acta* **1503,** 369–376
47. Finazzi, G. (2002) *Biochemistry* **41,** 7475–7482
48. Tandori, J., Baciou, L., Alexov, E., Maroti, P., Schiffer, M., Hanson, D. K., and Sebban, P. (2001) *J. Biol. Chem.* **276,** 45513–45515
49. Paddock, M. L., Feher, G., and Okamura, M. Y. (2003) *FEBS Lett.* **555,** 45–50
50. Hunte, C. (2001) *FEBS Lett.* **504,** 126–132
51. Gao, X., Wen, X., Esser, L., Quinn, B., Yu, L., Yu, C. A., and Xia, D. (2003) *Biochemistry* **42,** 9067–9080
52. Dikanov, S. A., Samoilova, R. I., Kolling, D. R., Holland, J. T., and Crofts, A. R. (2004) *J. Biol. Chem.* **279,** 15814–15823
53. Baciou, L., and Michel, H. (1995) *Biochemistry* **34,** 7967–7972
54. Soriano, G. M., and Cramer, W. A. (2001) *Biochemistry* **40,** 15109–15116
55. Allen, J. P., Feher, G., Yeates, T. O., Komiya, H., and Rees, D. C. (1988) *Proc. Natl. Acad. Sci. U. S. A.* **85,** 8487–8491
56. Hunte, C., Koepke, J., Lange, C., Rossmanith, T., and Michel, H. (2000) *Structure* **8,** 669–684
57. Kolling, D. R., Samoilova, R. I., Holland, J. T., Berry, E. A., Dikanov, S. A., and Crofts, A. R. (2003) *J. Biol. Chem.* **278,** 39747–39754
58. Stowell, M. H., McPhillips, T. M., Rees, D. C., Soltis, S. M., Abresch, E., and Feher, G. (1997) *Science* **276,** 812–816
59. Cramer, W. A., Zhang, H., Yan, J., Kurisu, G., and Smith, J. L. (2004) *Biochemistry* **43,** 5921–5929
60. Elbehti, A., Brasseur, G., and Lemesle-Meunier, D. (2000) *J. Bacteriol.* **182,** 3602–3606